ChemPhysChem

Research Article
doi.org/10.1002/cphc.202400767

Chemistry Europe
European Chemical Societies Publishing

www.chemphyschem.org

Electrophoretic Deposition of Carbon-Ionomer Layers on Proton Conducting Membranes

Michael Bredol,*[a] Ivan Radev,*[b] Giulia Primavera+,[a] Thomas Lange+,[b] Adib Caidi,[b] and Volker Peinecke[b]

Synthetic and natural carbons are widely used as carrier for electrodes in electrochemical applications. They need to have a controlled morphology in order to facilitate mass and charge transport, so the process of film formation is of uttermost importance. Here we show, how carbons (after proper preconditioning) can be codeposited with an ionomer by electrophoretic deposition, a method that does allow full control of deposition conditions during the process. In view of potential applications, we focus on the direct deposition on proton-conducting membranes. Ionomers and membranes applied are based on established per-fluorinated polyethylene with SO_3H-terminated side chains (PFSA). Conditions for reproducible deposition are reported in terms of optimal charge on the carbon particles, field strength in the deposition cell and necessary deposition times for a given film thickness. Additionally, a horizontal cell arrangement is suggested to avoid gravitational effects.

Introduction

Fuel cells as well as electrolyzers for H_2 generation need electrodes providing a three-phase-contact between an ion conductor, an electron conductor and a reagent. In most cases this is accomplished by the use of porous layers prepared from graphitized carbon nanomaterials (with anodes for water electrolysis being a notable exception), decorated with an ionomer and (if needed) an electrocatalyst. In the case of PEMFCs (proton exchange membrane fuel cells) this complex electrode system at a thickness of approximately 10–20 μm has to be deposited on or fixed to an ion-conducting membrane, separating the two half cells of the system. Deposition procedures used routinely for this purpose are for instance spraying or printing, needing dispersions or pastes of the decorated carbon particles. Such techniques are well suited for layers with uniform structure, but do not allow to vary the structure of the deposit during the process of deposition, e.g. for layers with gradients in their properties, or other superstructures as needed for advanced electrochemical applications.[1,2]

This report describes how electrophoretic deposition (EPD) can be applied for the carbon layer deposition step, opening ways to vary deposition conditions continuously during the process of layer formation, simply by variation of the electric parameters. EPD has found already large scale industrial use for instance in corrosion protection of metallic car bodies, but the mechanistic details are still somewhat unclear,[3–5] although the necessary coupled electroosmotic flow patterns have been modelled in order to better understand the deposition mechanism.[6] EPD is being driven by a strong electric field – therefore, we can also expect to find order and structure in deposited films, for instance when applying nanorods or other non-spherical particles.[7–11] Consequently, there are already reports on how to apply a special carbon variant, namely graphene, by EPD for electrochemical application.[12]

Moreover, direct deposition of carbon on a proton conducting membrane needs to overcome a specific obstacle, namely the electronically insulating character of the membrane – generally, EPD needs an electronically conducting substrate for electric field control as well as for charge balance. In the literature, this issue often has been resolved by the use of conductive primers,[13] but this is not a useful option for electrochemically active membranes with their open pore system.

EPD does also allow to control the morphology of the growing deposit[14] – it has even been used for the deposition of single nanoparticles, or on templated substrates in order to form arbitrarily structured films.[15] Another attractive option of EPD for electrochemical application is the fabrication of functionally graded films.[16]

In this report, we will focus on proton-conducting membranes for low temperature fuel cells with their need for a perfectly structured catalytic layer – membrane arrangement.[17–19] The state-of-the-art ionomer and membrane (mostly known under the brand name of Nafion® (DuPont), but there are also other names and manufacturers) is based on per-

[a] Prof. Dr. M. Bredol, G. Primavera+
FH Münster University of Applied Sciences
Department of Chemical Engineering
Steinfurt, Germany
E-mail: bredol@fh-muenster.de

[b] Dr. I. Radev, Dr. T. Lange,+ A. Caidi, Dr. V. Peinecke
ZBT GmbH, The Hydrogen and Fuel Cell Center
Duisburg, Germany
E-mail: I.Radev@zbt.de

[+] These authors contributed equally.

fluorinated polyethylene, substituted with SO_3H-terminated side chains (PFSA). In the membrane, these acidic side chains lead to swellable self-assembled proton-conducting channels, whereas the soluble variants are able to adsorb to carbon particles and other hydrophilic materials thanks to their very acidic terminal groups, providing colloidal (meta-) stability.

Colloidal stability is a critical condition for EPD – dispersions need to be stable enough to avoid aggregation and sedimentation, but must not be too stable as they need to form solid deposits when hitting the substrate surface. Regardless of the technique used the final morphology of the film and, therefore, its functionality in electrochemical applications will be influenced massively by the colloidal state of the precursor ink.[20] The stabilization method should be preferentially of electrostatic character, since sufficient electrophoretic mobility needs charges adsorbed to the particle surface (which subsequently of course need to be stripped off in the process of layer formation). In order to characterize the surface charge, the ζ-potential is employed quite often. Although this helps in many instances, one should keep in mind, that the relation between the number of surface charges and the measured potential is not always clear and may be even non-linear, especially in the presence of large electric fields.[21]

Another critical issue in EPD is overall electrochemical stability: voltages sometimes as high as 100 V are applied to the deposition cells, leading to extremely high electric potentials at the electrodes. In aqueous deposition systems this can lead to H_2- as well as O_2-evolution, disturbing structure formation or even leading to chemical decomposition processes in the dispersion used. Effects like this can either be suppressed by working in electrochemically inactive organic solvents (typically alcohols) or by pulsed deposition in order to suppress bubble formation.[22] Pulsed EPD may also help to form uniform and homogeneous deposits,[23–26] because the electroosmotic flow stops between pulses, allowing for free lateral movement of the depositing particles.[27]

The choice of the counter electrode is also critical: low temperature electrochemical processes depend very much on electrocatalytic activity, so counter electrodes with high overpotentials against water decomposition often prove to be helpful. In this report, the deposition of negatively charged carbon particles on a positive electrode will be investigated – the working electrode thus will be exhibiting a high positive electric potential. This is fortunate, because O_2-evolution as the result of water oxidation (the kinetically more complex process) is typically much slower than H_2-evolution and thus not only reduces the overall electrolytic current, but also reduces potential problems with bubble formation in the growing deposit simply by the fact, that the amount of oxygen developed stoichiometrically is always only half the amount of hydrogen. In the context of this manuscript, we will investigate deposition from carbon dispersions in isopropanol (IPA) with varying water contents and assume that electrolytic effects of the organic solvent will be even slower than water electrolysis.

Using anodic deposition on an ionic conductor also influences the mechanism of deposition: kinetically hindered water oxidation means, that the pH in the neighbourhood of the anode is not affected too much by electrochemical reactions – very much in contrast to the case of cathodic deposition on a metal electrode.[28] Deposition for the case discussed in this report rather means, that the travelling negatively charged carbon particles will experience double layer distortion followed by neutralization when hitting the surface – probably buffered by the protons available in the membrane.

EPD works best on electron-conductive substrates and has been demonstrated already for Pt-functionalized carbon deposits.[29] However, it is possible on non-conducting substrates as well, for instance when a thick dielectric deposit is being formed, which then serves as substrate for further deposition. Adjustment of voltages and pulses will be necessary in these cases, to overcome the steadily increasing isolating behaviour of the substrate,[30] but replenishment of the deleted source may also be effective.[31] EPD has also been used to create transparent coatings on conductive glass with metal atom clusters, producing compact, homogeneous assemblies with enhanced UV-NIR absorption and high visible transparency in under 90 seconds, demonstrating its industrial potential. Polymer binders stabilize metal clusters, enabling applications in optoelectronics, sensors, and catalysis.[32] In our case, ionomer binders, essential for PEMFCs, were employed to improve coating dispersion stability. In the present report, we will use proton-conducting membranes as substrates (Nafion®) mounted on (removable) metal stripes. This combination assures on the one hand a homogeneous electric field in the deposition region, but does (due to the mobile protons) also allow for active charge balancing without the need of redox activity.

EPD can also be used to form deposits of composites – either by homogeneous heterocoagulation and subsequent deposition, or by real co-deposition of solid particles.[33] The latter case needs a well balanced pattern of surface charging (of course of the same sign) in order to avoid preferential deposition of one component. Codeposition from dispersions containing nanoparticles and an organic resin or biochemical binder have been described already.[34,35] In our case here we will try to codeposit (Nafion®-) stabilized negatively charged carbons along with free Nafion®-polymer (actually aggregates[36,37]) from dispersion (often called a "ink"). Such a mixed dispersion with larger (carbon) and smaller (free Nafion®) particles will not only undergo electrostatic interaction between its components, but also show depletion contributions – a seemingly attractive force between the larger particles caused by entropy gain of the smaller ones.[38] When depositing two materials with different size and charge from a uniform dispersion, some segregation can be expected due to different electrophoretic mobilities. Following the treatment by Zhang et al.[15] and the references within that paper, the electrophoretic velocity v of a spherical particle with radius r, mass m and charge q in an electric field with strength E can be estimated as a function of time according to Eq. (1) (with η being the viscosity of the medium):

$$v = \frac{qE}{6\pi r\eta}\left[1 - \exp\left(-\frac{6\pi r\eta t}{m}\right)\right] \quad (1)$$

Figure 1 shows, that for particle sizes in the range interesting for electrochemical application it takes only some dozen nanoseconds to reach a stationary velocity, which (depending on charge, size and field strength) lies in the range of some μm/s. For typical deposition times of 10–20 min, this means that particles from a distance of up to some millimeters can reach the surface of the substrate – at a desired thickness of the deposit of 10–20 μm. Free Nafion® particles in dispersion will be much smaller and, therefore, reach much higher stationary velocities, but at the same time will be more strongly affected by random Brownian motion. The ratio of electrophoretic movement to Brownian movement can be estimated from Péclet's number *Pe*.[15] Again for spherical particles it can be estimated as shown in Eq. (2):

$$Pe = 12\frac{\varepsilon_r\varepsilon_0\pi}{k_B T}\zeta E r^2 \quad (2)$$

With a typical ζ-potential of −35 mV, the permittivity $\varepsilon_r\varepsilon_0$ of isopropanol, a temperature *T* of 298 K and a field strength *E* of 6 kV/m (k_B is Boltzmann's constant) we find values of *Pe* of about 3 and 12 for particles with radius 100 nm and 200 nm, respectively – at $Pe \gg 1$ movement is dominated by electrophoretic action. At 10 nm radius however (estimate for free Nafion® particles), *Pe* is on the order of 0.03 – with $Pe \ll 1$ these particles will undergo a lot of random Brownian motion competing with electrophoretic movement. We can therefore expect, that carbon particles will be deposited in a much more directed fashion than the free polymer when forming the codeposit. The primary aggregates of most synthetic carbons are not spherical, but slightly ellipsoidal. Therefore, most probably they are travelling preferentially with their longer axis oriented in the direction of the electric field at minimized hydrodynamic resistance.

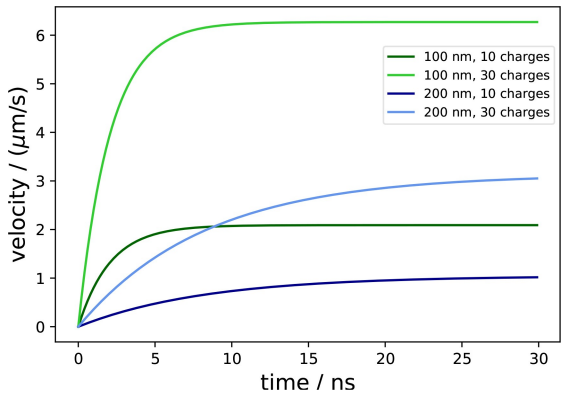

Figure 1. Electrophoretic velocity of spherical particles with the density of graphite, dispersed in isopropanol and accelerated by an electric field with strength 6 kV/m, according to Eq. (1).

Results and Discussion

Deposition runs on substrate samples with small area were performed with a simple vertical arrangement of counter electrode and working electrode. Figure 2 shows the overall appearance of a well adhering layer with columnar structure and homogeneous thickness after such a standard run at 60 V cell voltage, one centimeter electrode distance, 15 min deposition time, and using a quite thick and rigid Nafion® membrane as substrate. Such a membrane is mechanically quite stable, enabling easy handling and only minor deformation during further drying. EPD was tried under similar conditions also on Teflon® substrates, but without success, even after preconditioning in strong acids or oxidants – either charge balance or adherence of the first layer are hindered, probably because ions can not be exchanged with the substrate in this case.

The deposition ink included free Nafion® (partially adsorbed on the carbon particles), the deposit thus contains Nafion® as well. Successful codeposition (as needed for instance in fuel cells and water electrolyzers) was quantified with the help of EDX-spectroscopy (on cross sections) as well as FTIR spectroscopy on the layers. The latter method did not need destruction of the sample, but could work only for thicker layers, because the substrate (membrane) was composed of Nafion® as well. It turned out, that the ratio of Nafion® to carbon deposited depends on the deposition conditions – with increasing cell voltage (and decreasing deposition time for a given thickness target) the amount of fluorine detected in the layer became much smaller, up to a factor of approximately 10 when switching from 40 V to 80 V (see Table 1 for an example run).

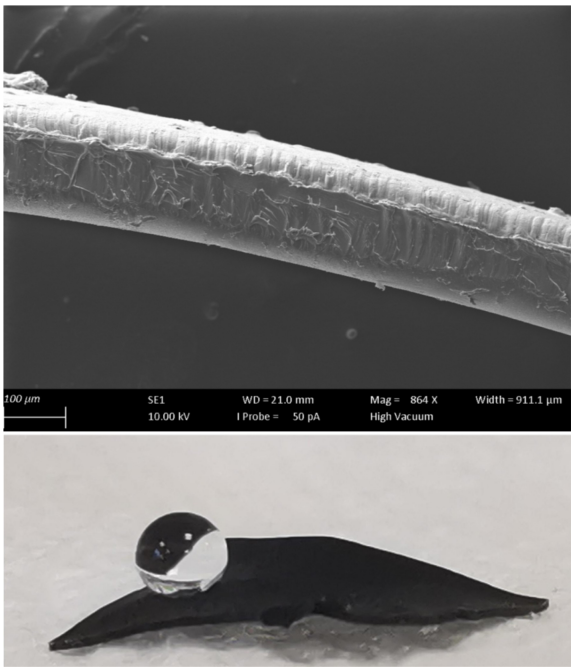

Figure 2. EPD of PFSA-stabilized Vulcan® carbon under DC conditions (60 V for 15 minutes) on a Nafion® membrane. Top: overall appearance (top layer: carbon), scalebar: 100 μm. Bottom: hydrophobicity demonstrated by a drop of deionized water.

Table 1. Exemplary variation of F-content with cell voltage as measured by FTIR/ATR spectroscopy.

cell voltage/V	deposition time/min	ionomer content/mass %
80	10	3.8
60	20	23.4
40	30	38.3

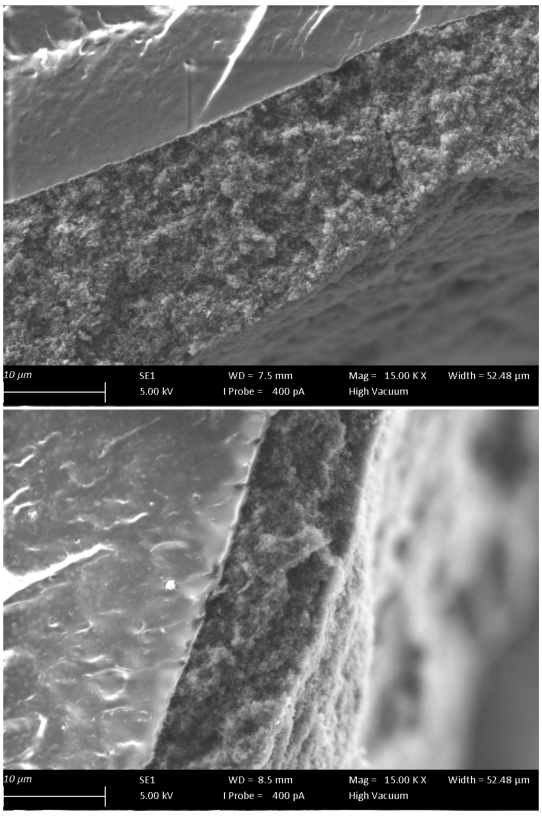

Figure 3. EPD of PFSA-stabilized Ketjen® blacks on a thick Nafion® membrane, scalebar: 10 µm. Top: Ketjen® EC-300J (membrane in upper part). Bottom: Ketjen® EC-600JD (membrane on left side).

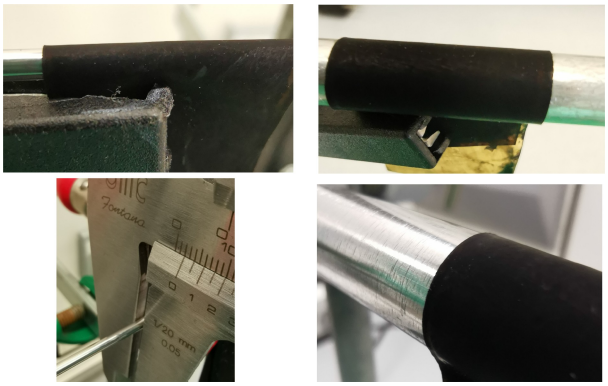

Figure 4. Mandrel bend tests with Ketjen® EC-600JD deposits. Mandrel diameter: 2 mm (top left), 6 mm (top right) and 12 mm (bottom right), together with the 2 mm mandrel in a caliper (bottom left).

This effect may be due to the higher overall charge and thus migration mobility of the carbon particles, as compared to the single ionomer entities.

Figure 3 shows the structure of the deposits at higher magnification, using two variants of Ketjen® blacks (EC-300J and EC-600JD). In order to test the mechanical stability of the layers, cylindrical mandrel bend tests (following the spirit of DIN EN ISO 1519) were performed with a series of mandrels between 12 mm and 2 mm diameter. After forcing the flexible deposit/membrane system around the mandrel under test, Figure 4 shows for a sample with Ketjen® EC-600JD deposits the appearance of the layer systems for three mandrel diameters, including the thinnest one – no cracks or peel-off was observed, proving a mechanical stability high enough for use in e.g. fuel cell stacks.

The thickness of the deposited layer depends on the nature of the membrane (manufacturer and thickness), the colloidal properties of the ink and of course on time and field strength during EPD. Figure 5 shows, how varying time and applied voltage may change the thickness easily over dozens of micrometers. Especially the cell voltage can easily be changed during deposition by employing a function generator coupled to the power amplifier – be it as a simple ramp or in the form of pulses. This possibility opens a large parameter room for manipulation of layer properties during deposition in a graded manner.

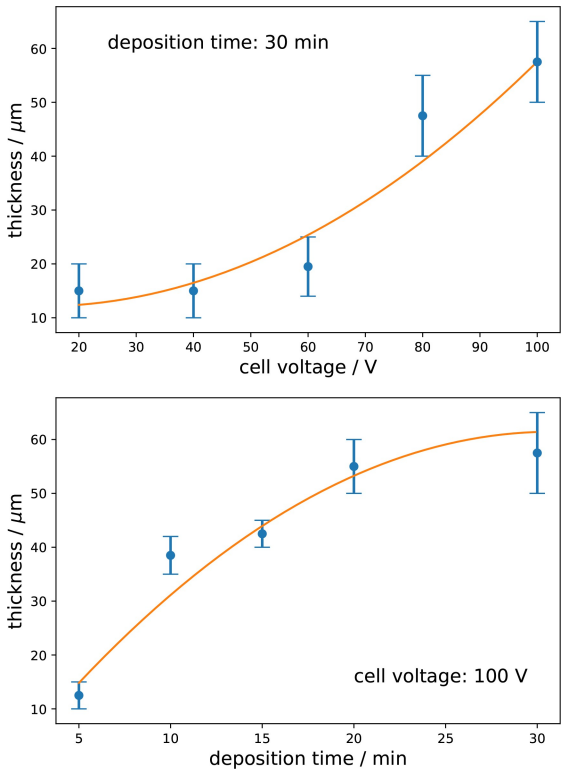

Figure 5. Influence of deposition parameters for EPD on a thick Nafion® membrane. Top: varying cell voltage at 30 min deposition time. Bottom: varying deposition time at 100 V cell voltage. Electrode distance 1 cm in both cases. Errorbars estimated from repeated measurement, orange lines: parabolic trends.

For larger substrates, however, it turned out, that sedimentation effects of larger aggregates in the dispersion led to an uneven thickness of the deposit. Therefore, a horizontal electrode holder was developed and fabricated from PETG (polyethylene terephthalate glycol) by 3D-polymer-printing, now allowing for deposition runs on membranes up to 2×4.5 cm^2 without disturbance, see Figure 6. The working electrode now was mounted above the counter electrode with the effect that sedimenting larger aggregates could not reach it. As an immediate effect, film thicknesses tend to be smaller as compared to the vertical cell, simply because larger aggregates now sediment and are therefore not deposited by EPD on the top electrode.

Keeping in mind, that a typical thickness of an electrode layer in a fuel cell is on the order of 10 μm, runs using the horizontal cell were performed with varying cell voltages and deposition times, exploring the parameter space available. Figure 7 depicts, how the film thickness is varying with voltage and time, always showing thickness increase with time as well as voltage. The carbon variant used in this case was non-pretreated Ketjen® EC-300J, which appeared to possess sufficient colloid chemical stability without further oxidation. Disturbing the original surface conditions by further oxidation with this material led to more instable dispersions – deposition runs then led to inhomogeneous films and loss of the clear relations between thickness and deposition parameters as visible in Figure 7.

In order to find out the most favourable colloidal conditions for controllable EPD, ζ-potential and particle size measurements were performed for all inks preferred. As outlined in the introduction, it turned out, that there is a stability window suited for EPD – it is situated in the range between −30 mV and −40 mV ζ-potential. In this range, the particle size as characterized by DLS (dynamic light scattering) is found to be on the order of the primary aggregate size (ca. 250 nm). With absolute values of the ζ-potential smaller than 30 mV, the colloidal stability is too low, and larger aggregates are forming continuously in the ink, leading to ill-defined deposits. Absolute values of the ζ-potential larger than 40 mV on the other hand prevent deposition and adherence (due to strong repulsion between the particles in the ink), leading to very small or just zero deposition efficiency.

Other carbon variants can be used as well, always taking care of proper colloid chemical profile. With Vulcan® XC72 for instance pre-oxidation is necessary for proper behaviour under EPD conditions. Figure 8 shows, that the parameters again are related monotonically to layer thickness, but with different steepness. This means, that EPD has to be re-calibrated in terms of the thickness target for every combination of membrane and carbon variant – a general necessity well known from the literature, when applying EPD.

Using deposits prepared on larger substrates in the horizontal cell, conductivity measurements were performed in order to assess the suitability for electrochemical applications.

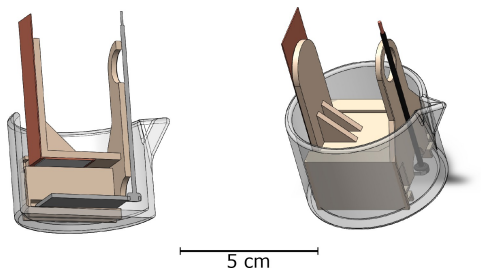

Figure 6. Construction of horizontal cell – bottom electrode made from stainless steel, top electrode made from copper strip, with membrane attached, cell 3D-printed in PETG to support counter and working electrode at a constant distance of 1 cm. Vessel (beaker) to be flooded with deposition ink.

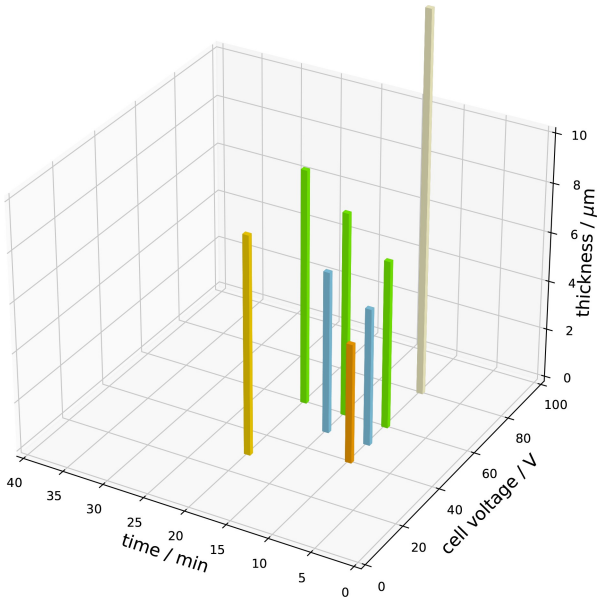

Figure 7. Influence of deposition parameters for EPD in a horizontal cell. Membrane: Nafion® 117 (supplier: Ion Power). Carbon variant: Ketjen® EC-300J (as received).

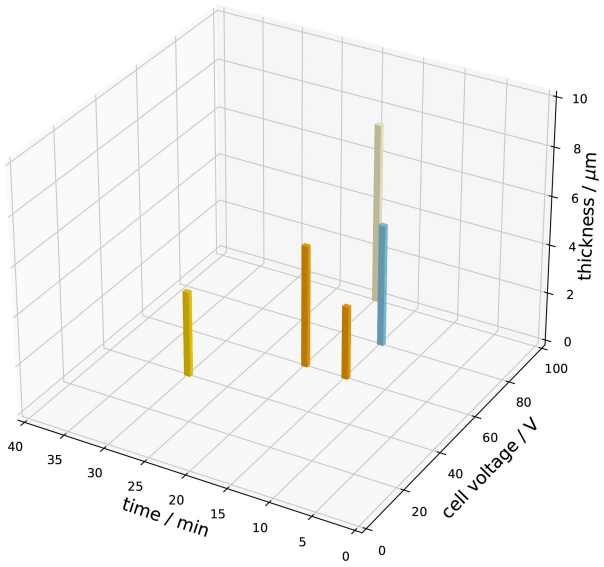

Figure 8. Influence of deposition parameters for EPD in a horizontal cell. Membrane: Nafion® 117 (supplier: Ion Power). Carbon variant: Vulcan® XC72 (preconditioned oxidatively).

As expected it turned out, that conductivity under AC conditions (reflecting the sum of electronic and ionic contributions) was higher than under DC (probing only electronic contributions) – the films obviously are co-deposits of carbon and Nafion® and show the necessary electronic conductivity along with ionic contribution. Moreover it turned out, that the (specific) conductivity was increasing with the cell voltage and deposition time – although it is difficult to differentiate between the effects of voltage and layer thickness. This behaviour points to different layer morphologies as a function of deposition conditions. From a series with Ketjen® carbons (variants EC-300J and EC-600JD) deposited on thick membranes at 60 V cell voltage for varying times in the horizontal cell configuration Figure 9 shows how the DC conductivity and the AC conductivity are trending with layer thickness – although thickness measurements are not always reliable, there is a trend for reduced conductivity with increasing thickness, perhaps by increasing porosity with increasing thickness.

Thinner membranes are more difficult to handle – they tend to deform massively under wetting and drying and thus need special care when being mounted and dismounted. Moreover, the relation between film thickness and EPD conditions changes markedly and had to be recalibrated – but similar effects even were observed when just changing the manufacturer. Obviously the details of the membrane have a huge influence on the deposition behaviour, pointing for instance to the differences in how the conductive channels in the membrane are arranged. As a general trend, thinner membrane substrates led to thicker layers – probably an effect of decreased resistance in the membrane and a thinner dielectric barrier on the electrode.

In practical applications (for instance in fuel cells) the layers will contain electrocatalysts, for instance based on nanoparticular Pt. In contact with fumes of a volatile solvent like IPA and air this may lead to combustion – an unwanted effect that may destroy the whole layer system. In order to avoid this, water is added to the IPA, decreasing the inflammability. To check out, whether EPD does work in the presence of some water, a series of experiments with increasing water addition to the ink was performed. As a result, it turned out, that up to 30 wt% of water was tolerated by the system – without gas evolution at the electrodes and without measurable currents. EPD thus may work safely also with highly active electrocatalysts.

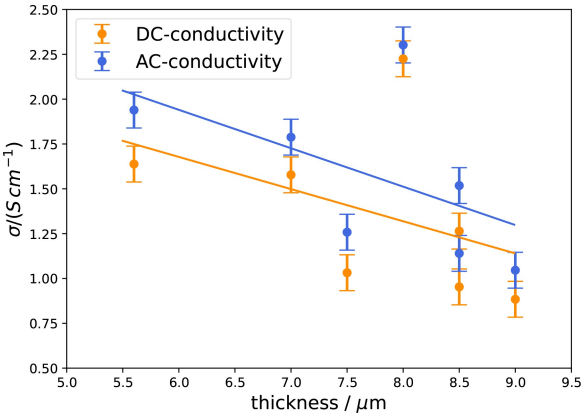

Figure 9. Trend of conductivity with thickness after EPD in a horizontal cell at 60 V. Membrane: Nafion® 117 (supplier: Ion Power). Carbon variant: Ketjen® (two variants).

Conclusions

In this work we have shown, that surface-modified carbons and PFSAs can be codeposited by EPD directly onto a Nafion® membrane. The layers formed are mechanically stable, often show a columnar structure and are strongly adhering to the substrate. Gravitational effects on larger substrates can be avoided by using horizontal electrode arrangements with EPD working against gravitation. Dispersions of carbons and PFSAs in IPA suited for controllable EPD were characterized by $-40\,\text{mV} < \zeta < -30\,\text{mV}$. Deposition voltage and deposition time under these circumstances are reproducible for one kind of carbon and membrane, but need to be readjusted when the kind of membrane or carbon is changed. Nevertheless, the ζ-potential as a simple measure proved to be a powerful indicator for suitability of an ink, for instance when exploring electrocatalyst powders with in many cases unknown surface properties. The AC (1.0–2.3 S cm^{-1}) and DC (0.9–2.2 S cm^{-1}) conductivity measurements at the optimised EPD voltage of 60 V provide evidence that these layers are suitable for use in proton exchange membrane water electrolyzer (PEMWE) cathodes and PEMFC electrodes. The discrepancy between the AC and DC conductivities corroborates the EDX and FT-IR findings, which indicate that during EPD, an ionomer is deposited alongside the catalyst support. This is significant for the formation of optimized electrochemically active surface area and for the adhesion of the EPD layers to the PEM (for instance Nafion®), as well as for their mechanical stability. These findings demonstrate the potential of EPD to create layers with desired characteristics, including ionomer/carbon ratio, porosity, and conductivity. Based on these encouraging outcomes and optimized EPD parameters, future research will focus on EPD of Pt-containing catalyst layers and their electrochemical evaluation in PEMFCs.

Experimental

Carbon powders used were either VulcanXC72® (Cabot) or Ketjen® blacks (variants EC-300J and EC-600JD). In order to create particles with primarily hydroxyl or carboxyl surface groups, surface modifications were performed with H_2O_2 (Carl Roth, 10 wt%). In a typical experiment, 120 mg of carbon powder was dispersed in 100 mL solution of the oxidizing agent. The mixture was introduced into a round bottom flask and refluxed under continuous stirring for 3 h. The functionalized carbons were diluted with deionized water and then thoroughly filtered and washed. The received materials were then dried in an oven at 110 °C overnight. After the preconditioning process, ζ-potential and particle size analysis were performed (Zetasizer Nano ZS, Malvern Instruments). It became evident that, whereas Vulcan® XC72 and Ketjen® EC-600JD had benefited from the pre-treatment in terms of colloidal stability of the ink, the dispersion made with Ketjen ®EC-300J resulted in a

lower absolute value of the ζ-potential and bigger particle agglomerates. Therefore, the latter material was used in further experiments as received without pre-conditioning.

All carbon dispersions were prepared in isopropanol (IPA). In a typical run 15 mg of the chosen carbon powder (Vulcan® XC72, Ketjen® EC-300J, or Ketjen® EC-600JD) was added to 30 mL IPA (Carl Roth), alongside with a 5 wt% Nafion® D521 (1100 EW) aqueous solution (Chemours). The dispersions were prepared with 75 mg of ionomer solution to obtain Nafion® concentrations of 20 wt% with respect to the total mass of solids in the ink. When testing the overall water tolerance of the system, additional deionized water was added.

In order to generate a uniform electric field, the Nafion® membranes were mounted on a flexible copper strip with the help of a conductive glue (sourced from TRU components), that could be removed completely after the experiment. Prior to mounting, the membranes were soaked for at least 30 min in pure IPA and then immediately transferred to the cell (after removal of free excess liquid).

For EPD, a Kepco bipolar power amplifier was used as the voltage source. The counter electrode was made from AISI 316, an austenitic chromium nickel steel with very high resistance against corrosion. With carbon and Nafion®-particles being negatively charged, deposition took place on the positive electrode. After deposition, the copper strip was removed, and the films were dried first in air, and then in a vacuum cabinet at slightly elevated temperature.

In order to quantify the amount of material deposited during EPD, a simple gravimetric analysis was performed. The samples were dried before a deposition run in a vacuum oven at 80 °C for 4 h to remove absorbed water, weighted after cooling and then stored between two glass plates. After the deposition process, the membrane underwent the same drying and weighting procedure, using the weight difference for further analysis.

The microstructure of the deposited layers was analyzed with a Zeiss EVO MA19 scanning electron microscope with energy dispersive X-ray analyzer (EDX). Coated membranes were broken by cryogenic fracture after immersion in liquid nitrogen for a few minutes.[39]

FTIR spectra for the determination of the amount of fluorine in the deposited layers were collected on a Nicolet iS5 equipped with a iD5 diamond crystal for attenuated total reflection (ATR) in the range 4000 to 650 cm^{-1} (averaged over 50 scans with a resolution of 0.121 cm^{-1} and background correction). A calibration curve was prepared from a range of samples of known concentration of ionomer in carbon, in a range from 0 to 40 wt%. Pure Nafion® was taken as reference, and the assignment of the vibrational bands was based on literature data.[40–42] The CF_2 asymmetric stretching band at ca. 1200 cm^{-1} was used for quantification of the ionomer in the layer, based on peak height and peak area. To obtain reliable results, it was important to ensure that the IR radiation penetrates only the carbon layer and does not reach the membrane below. With the refractive indices of the diamond crystal (2.4), the sample (between 1.23 for pure Nafion® and 1.36 for pure carbon), and the angle of incidence of the IR beam the penetration depth was estimated as 4–6 μm. Therefore, only layers with a thickness larger than 6 μm were investigated with this approach.

Electrical characterization of the films was performed in a home-built apparatus by a four electrode measurement principle in in-plane direction at ambient conditions. All electrodes were gold-plated and pressed mechanically to the films. Working and counter electrodes were strip-like and applied in parallel. The apparatus is equipped with two pairs of sense electrodes, which enable the simultaneous measurement of electrical activity at two distinct points within the layer. AC conductivity was measured by electrochemical impedance spectroscopy (EIS) in the frequency range of 4 MHz to 1 Hz at open circuit voltage with a 5 mV sinusoidal perturbation. The results were found to be consistent regardless of whether a potential difference of 5 or 10 mV was applied.

Acknowledgements

Acknowledgements are due to Thomas Jüstel (Department of Chemical Engineering, FH Münster) for providing access to electron microscopy. Open Access funding enabled and organized by Projekt DEAL.

Conflict of Interests

The authors declare no conflict of interest.

Data Availability Statement

The data that support the findings of this study are available from the corresponding author upon reasonable request.

Keywords: proton conducting membranes · electrophoretic deposition · carbon

[1] Z. Song, L. Miao, Y. Lv, L. Gan, M. Liu, *J. Mater. Chem. A* **2023**, *11*, 12434.
[2] Z. Xie, T. Navessin, K. Shi, R. Chow, Q. Wang, D. Song, B. Andreaus, M. Eikerling, Z. Liu, S. Holdcroft, *J. Electrochem. Soc.* **2005**, *152*, A1171.
[3] L. Besra, M. Liu, *Prog. Mater. Sci.* **2007**, *52*, 1.
[4] B. Giera, L. A. Zepeda-Ruiz, A. J. Pascall, T. H. Weisgraber, *Langmuir* **2017**, *33*, 652.
[5] P. Sarkar, P. S. Nicholson, *J. Am. Ceram. Soc.* **1996**, *79*, 1987.
[6] G. Falk, *J. Phys. Chem. B* **2013**, *117*, 1527.
[7] A. Singh, N. J. English, K. M. Ryan, *J. Phys. Chem. B* **2013**, *117*, 1608.
[8] T. Lin, S. M. Rubinstein, A. Korchev, D. A. Weitz, *Langmuir* **2014**, *30*, 12119.
[9] T. Prasse, L. Flandin, K. Schulte, W. Bauhofer, *Appl. Phys. Lett.* **1998**, *72*, 2903.
[10] M. Trau, D. A. Saville, I. A. Aksay, *Langmuir* **1997**, *13*, 6375.
[11] T. D. Edwards, M. A. Bevan, *Langmuir* **2014**, *30*, 10793.
[12] A. Chavez-Valdez, M. S. P. Shaffer, A. R. Boccaccini, *J. Phys. Chem. B* **2012**, *117*, 1502.
[13] P. M. Vilarinho, Z. Fu, A. Wu, A. Axelsson, A. I. Kingon, *Langmuir* **2015**, *31*, 2127.
[14] K. R. Panta, C. A. Orme, B. N. Flanders, *J. Colloid Interface Sci.* **2023**, *636*, 363.
[15] H. Zhang, Y. Liu, Y. Dong, A. Ashokan, A. Widmer-Cooper, J. Köhler, P. Mulvaney, *Langmuir* **2024**, *40*, 2783.
[16] M. A. Salazar de Troya, J. R. Morales, B. Giera, A. J. Pascall, M. A. Worsley, R. Landingham, W. L. Du Frane, J. D. Kuntz, *Mater. Des.* **2021**, *209*, 110000.
[17] I. Fouzaï, S. Gentil, V. C. Bassetto, W. O. Silva, R. Maher, H. H. Girault, *J. Mater. Chem. A* **2021**, *9*, 11096.
[18] K. Jiao, J. Xuan, Q. Du, Z. Bao, B. Xie, B. Wang, Y. Zhao, L. Fan, H. Wang, Z. Hou, S. Huo, N. P. Brandon, Y. Yin, M. D. Guiver, *Nature* **2021**, *595*, 361.
[19] S. Sui, X. Wang, X. Zhou, Y. Su, S. Riffat, C.-j. Liu, *J. Mater. Chem. A* **2017**, *5*, 1808.

[20] M. Bredol, A. Szydło, I. Radev, W. Philippi, R. Bartholomäus, V. Peinecke, A. Heinzel, *J. Power Sources* **2018**, *402*, 15 .
[21] D. V. Matyushov, *J. Phys. Chem. B* **2024**, *128*, 2930.
[22] A. Chávez-Valdez, A. R. Boccaccini, *Electrochim. Acta* **2012**, *65*, 70.
[23] B. Neirinck, O. Van der Biest, J. Vleugels, *J. Phys. Chem. B* **2013**, *117*, 1516.
[24] M. Ammam, *RSC Adv.* **2012**, *2*, 7633.
[25] M. N. Naim, M. Iijima, H. Kamiya, I. W. Lenggoro, *Colloids Surf. A* **2010**, *360*, 13.
[26] B. Neirinck, J. Fransaer, O. Van der Biest, J. Vleugels, *Electrochem. Commun.* **2009**, *11*, 57.
[27] M. N. Naim, M. Iijima, K. Sasaki, M. Kuwata, H. Kamiya, I. W. Lenggoro, *Adv. Powder Technol.* **2010**, *21*, 534.
[28] T. Uchikoshi, *J. Ceram. Soc. Jpn.* **2024**, *132*, 387.
[29] A. Szydło, J.-D. Goossen, C. Linte, H. Uphoff, M. Bredol, *Mater. Chem. Phys.* **2020**, *242*, 122532.
[30] M. Bredol, J. Micior, S. Klemme, *J. Mater. Sci.* **2014**, *49*, 6975.
[31] P. Tiwari, N. D. Ferson, D. P. Arnold, J. S. Andrew, *Front. Chem.* **2022**, *10*.
[32] N. T. K. Nguyen, A. Renaud, B. Dierre, B. Bouteille, M. Wilmet, M. Dubernet, N. Ohashi, F. Grasset, T. Uchikoshi, *Bull. Chem. Soc. Jpn.* **2018**, *91*, 1763.
[33] J.-D. Goossen, A. Alizade, M. Bredol, *Mater. Chem. Phys.* **2020**, *239*, 122083.
[34] Y. Iso, S. Takeshita, T. Isobe, *Langmuir* **2014**, *30*, 1465.
[35] M. Akram, N. Arshad, M. K. Aktan, A. Braem, *ACS Appl. Bio Mater.* **2020**, *3*, 7052.
[36] H. Srivastav, A. Z. Weber, C. J. Radke, *Langmuir* **2024**, *40*, 6654.
[37] H. Srivastav, A. Z. Weber, C. J. Radke, *Langmuir* **2024**, *40*, 6666.
[38] G. Onuh, D. Harries, O. Manor, *Langmuir* **2024**, *40*, 8554.
[39] F. Ma, Y. Z. Zhang, X. L. Ding, L. G. Lin, H. Li, *Adv. Mater. Res.* **2011**, *221*, 37.
[40] C. Heitner-Wirguin, *Polymer* **1979**, *20*, 371.
[41] S. R. Lowry, K. A. Mauritz, *J. Am. Chem. Soc.* **1980**, *102*, 4665.
[42] J. Ostrowska, A. Narebska, *Colloid Polym. Sci.* **1983**, *261*, 93.

Manuscript received: August 2, 2024
Revised manuscript received: October 14, 2024
Accepted manuscript online: November 6, 2024
Version of record online: November 27, 2024